WIND TURBINE BLADES: MODIFICATIONS TO REDUCE AERODYNAMIC NOISE

A Technical Paper submitted to the Department of Mechanical
And Aerospace Engineering University of Virginia
MAE 4620: Machine Design II

Written By:

Megan Anderson

Nathan Jacobson

Levi Otis

Caleb Owen

Justin Smith

May 11, 2021

INTRODUCTION

Over the past decade, the social and political push to address environmental issues like pollution and climate change has driven industrial utilization of newer technologies. This shift combined with the growing demand for electricity has drawn attention to the importance of renewable energy, contributing to 19.8% of total domestic power generation in 2020 (Energy Information Administration [EIA], 2020). More specifically, the growth of wind power jumped 36.7% from 2010 to 2017 to account for 338 billion kilowatt-hours last year ([EIA], 2020).

The explosive development of wind power has emphasized another challenge to its acceptance within modern society: noise production. While the necessity for space has predominantly isolated the turbines to rural areas, its encroachment on local communities has been fraught with complaints due to the sound of the large blades. A panel of experts conducted research into the issue to establish a causal relationship between turbine noise and annoyance of nearby residents (Council of Canadian Academies, 2015). The study additionally suggested ties between sound and sleep disruption. Moreover, the noise disturbance acts as another barrier to the development of wind power by preventing turbines from pushing into more populated areas.

To address this issue, the objective of the project was to optimize the design of a horizontal axis wind turbine by reducing noise generation. Although the mechanical noise is especially harsh due to its tonal character, it has been largely mitigated through the implementation of sound-absorbent materials and nacelle shielding. Consequently, the objective focused on the optimization of rotor blade design to minimize aerodynamic noise that originates from the leading edge, trailing edge, and tip of the airfoil.

BACKGROUND

While mechanical noise stems from the generator, hydraulic systems, and the gearbox, aerodynamic noise derives from the turbulent airflow over the blades (Jianu, Rosen, & Naterer, 2012). The traditional NACA 2414 airfoil capitalizes upon its angle of attack to achieve the maximum lift force and cause the rotor to spin. The design fails, however, to address boundary layer separation and turbulent eddies responsible for aerodynamic noise.

This noise classification can be further divided into the subcategories of inflow turbulence, trailing edge, and tip noise. Trailing edge noise is considered the dominant component of total noise generation attributed to wind turbines. When the boundary layer interacts with the sharp trailing edge, the turbulent eddies that form produce the high pitch sound most commonly associated with the spinning blades (Deshmukh et al., 2019). Additionally, the trailing edge noise is most significant at higher velocities because the region of noise generation shifts towards the blade tip, where the airflow is the most turbulent (Deshmukh et al., 2019). Tip noise is generated by a mechanism similar to trailing edge noise, where a vortex formed from the pressure differential cross-flow interacts with the sharp tip edge and produces noise (Deshmukh et al., 2019). Lastly, inflow noise comes from the impact between the blade surface and the incoming air due to the presence of atmospheric turbulence (Buck, Oerlemans, & Palo, 2016).

Using the NACA 2414 airfoil as a reference for design and testing, the group developed three other blade designs to address each of the aerodynamic noise types. The modifications to the trailing edge rely on the proportionality relationship between sound scattering and eddy path; it indicates that noise generation is maximized when the flow follows a perpendicular path and drops off the trailing edge (Hall & Williams, 1970). Consequently, the blade design draws inspiration from the silent flight of the owl with its soft feathers that damp out the turbulence and

maintain a more laminar flow over the wing (BBC Earth, 2016). The base blade was modified to include a strip of flexible material cut into serrations along the trailing edge that reduces the flow path angle and theoretically reduces noise.

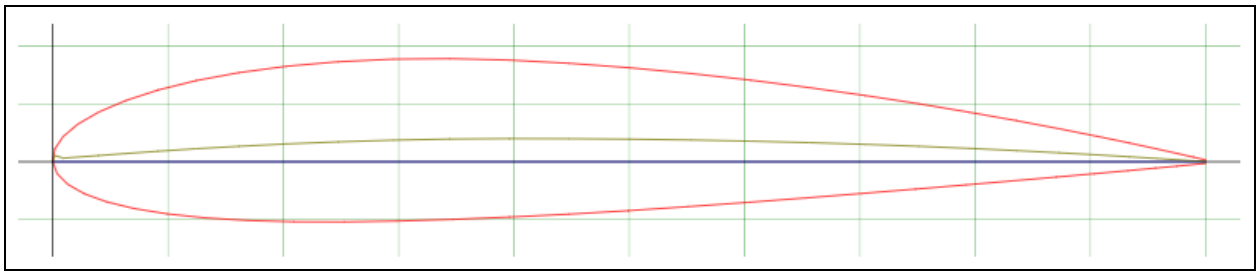

Figure 1. NACA 2414 airfoil (airfoiltools.com, 2020)

To mitigate tip noise, the new design aims to address the turbulent vortices formed from the interaction between the sharp blade tip and the pressure differential cross-flow (Deshmukh et al., 2019). Aircrafts have historically featured a curved wingtip to alter the vectors for the mixing pressure fields, effectively reducing the high pitch noise (Real Engineering, 2016). The modified turbine blade aims to address the issue in the same way, where the curvature is theorized to delay vortex separation and consequently minimize the sound.

The third design aspires to handle the unpredictable nature of turbulent inflow noise. Through further study of owls, the team observed that the birds possess noded feathers on the leading edge of their wings. These nodes are suspected to work by breaking up the incoming airflow. The resultant mixing increases the exchange of momentum to stabilize the boundary layer, ultimately reducing turbulent vortices that contribute to sound propagation (Deshmukh et al., 2019). Furthermore, the addition of raised bumps on the leading edge of the turbine blade is theorized to achieve a similar effect to the owl wing.

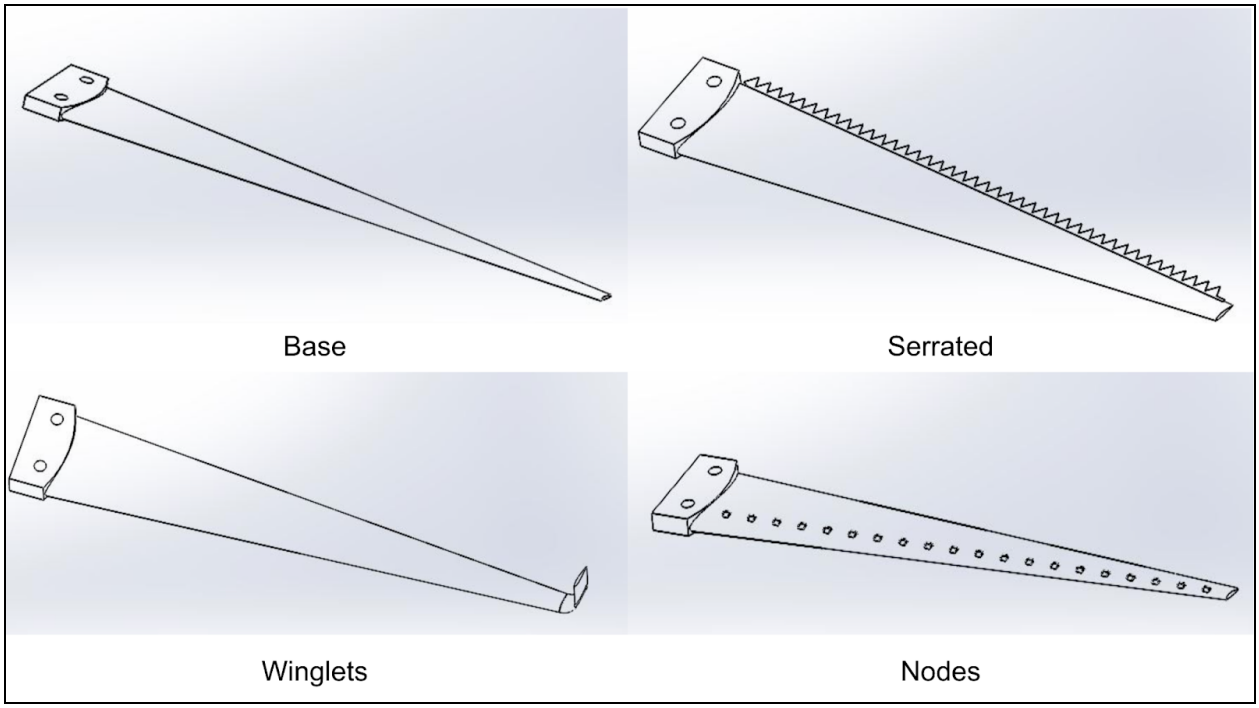

Figure 2. The four modified blade designs.

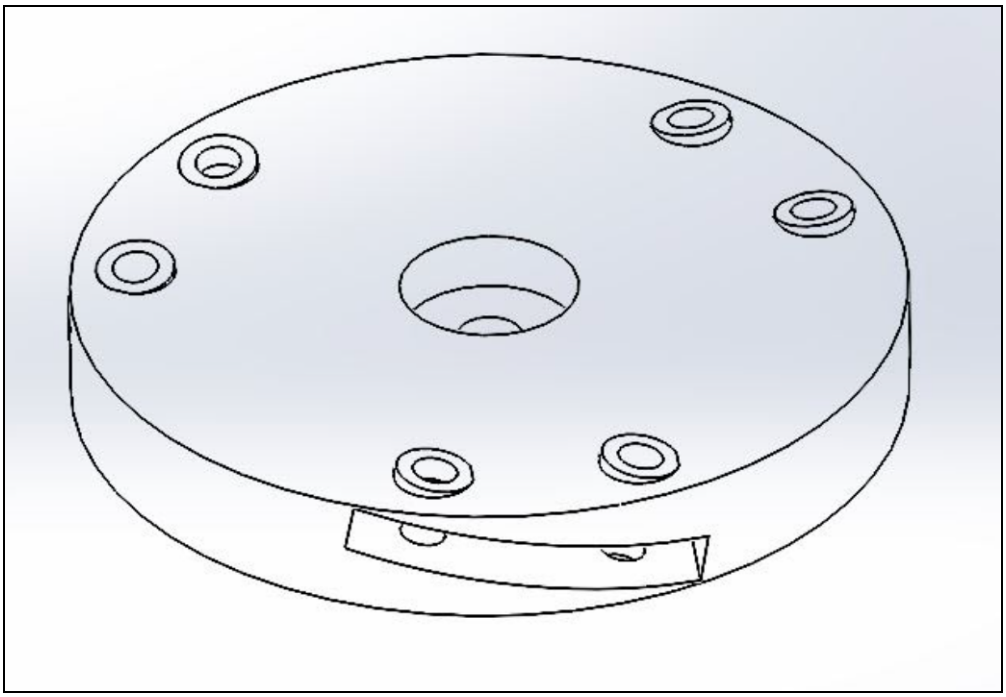

Figure 3. The final hub design with a 10° pitched slot.

SPECIFICATIONS

Aside from noise reduction, the project specifications outlined that the blade design maintained turbine power output, performed in high-stress environments, and remained low cost and easily manufacturable. While some research has indicated a potential trade-off between sound reduction and electricity generation, the team aimed to develop blades that minimized this compromise. Typical rotor blades are also expected to survive wind speeds of approximately 160 mph, making the durability specification imperative to any design. Moreover, the team decided to monitor the fabrication and overall cost of implementation to better address the potential barriers of wind turbine development within modern industry.

Calculations:

To measure the durability of the blades, the designs were subjected to structural analysis for safety before they were subjected to verification through physical trials. Although the drag coefficient for turbine blades hovers within the range of 0.1 to 0.5, it varies according to the angle of attack and velocity (Bai, et al., 2013). Consequently, a worst-case approximation of the critical force on the blades was calculated using the maximum drag coefficient and safety factor of 2. The calculation was performed according to the following equation (1), where C_D represents the drag coefficient, ρ the air density, A the frontal blade area, and V the wind speed. Each of the designs was evaluated in Solidworks for both 40 mph and 120 mph winds to ascertain that the blades would not exceed their yield stress nor deflect to an observable amount. These results relied on a fixed geometry and neglected gravity due to its insignificance compared to the centrifugal force for blades made out of ABS plastic (B-3 & B-4). While fiberglass was preferred for implementation given its significantly greater strength, it was not readily available in the software and the plastic modeled testing conditions of the scaled model most accurately.

$$F_D = \frac{C_D \rho A V^2}{2} \qquad (1)$$

$$a_c = \frac{v^2}{R} \qquad (2)$$

$$\omega = \frac{60 v_{tip}}{\lambda \pi D} \qquad (3)$$

The theoretical maximum angular velocity (3) was determined from a structural analysis of the blades. Using the critical force derived from material properties, the centripetal acceleration (2) was calculated for the center of mass of the blade to derive the tangential speed and then doubled to obtain the tip speed. A typical ratio of tip to wind speed ($\lambda = 6$) was employed to derive the maximum wind speed. Based on these approximate calculations, the theoretical maximum rotational speed was derived to exceed 2500 rotations per minute with an associated wind speed of 180 mph (B-5). On the other hand, the maximum stress under each wind condition did not exceed the yield strength approximated as 30 MPa within Solidworks, (B-2). The stress simulation for the winglet blade was included for verification (B-3 & B-4). Additionally, the deflections of the blades when subjected to 40 mph winds were all within two millimeters (B-2). At 120 mph, however, the deflections surpassed a considerable 10 millimeters, where the winglet design peaked at 128-millimeter deflection (B-2). These results were most likely due to high ductility attributed to the plastic in comparison to the more common fiberglass; the designs were considered safe since the wind tunnel was capped at 75 mph. Overall, the analysis indicated that the designs met the durability specification as shown by minimal deflection and tolerable stresses at 40 mph and 560 rpm (B-2).

Fabrication Process:

Following safety verification, the blades were all manufactured through the Rapid Prototype 3D Lab at the University of Virginia. The acceptable production timeline was an additional 2.25 days for the modified designs in comparison to the manufacture of the NACA

2414 airfoil. The modifications only added an extra day to the fabrication of all three sound mitigating designs, satisfying the ease of manufacture specification. However, the final set of blades required multiple attempts to manufacture since the limits of the printer were not taken into account in the original part files. For example, the initial thicknesses of the serrations, nodes, and winglets were below the threshold of the printer and yielded defective blades (Figure 4). As a result of these limitations, the trailing edge modification was added using adhesive to secure a hand-cut strip of serrations; the other designs were reprinted (Figure 5). The impact of the team's unfamiliarity with the printing process, although significant to the overall process, was not taken into account in the evaluation of the manufacturability specification.

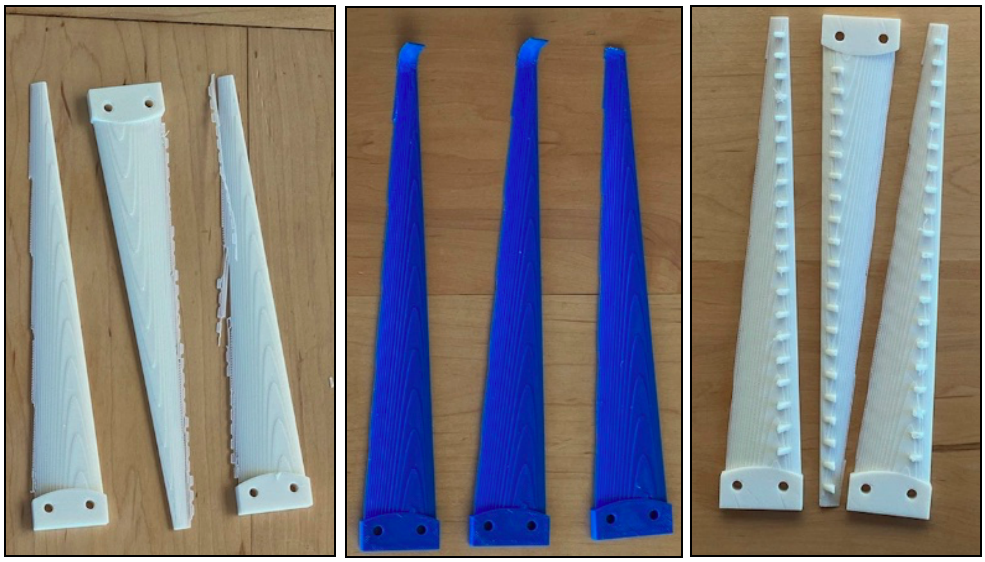

Figure 4. The initial set of modified blade prints to illustrate low quality; pictured from left to right: serrations, folded tips, nodes.

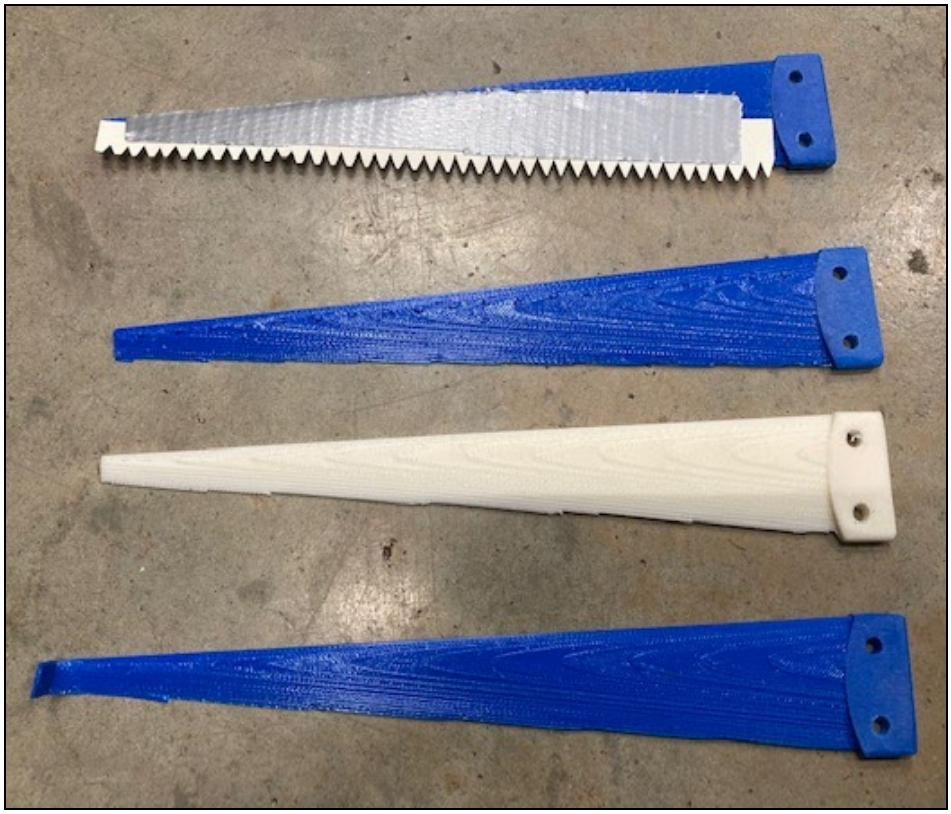

Figure 5. The final set of modified blade prints; pictured from top to bottom: serrations, nodes, base, winglets.

Similarly, the numerous attempts to print functional blades impacted the overall cost attributed to each of the designs. The initial set of blades did not vary in cost significantly from the base blades; the folded tip and node sets actually cost less than the control design (C-1). Although the first set of these modified blades fell within the additional 5% cost threshold compared to the original airfoil, the design with a serrated trailing edge did not meet the specification. Additional material to draw the serrations accounted for the extra $4.59 to manufacture this design and push the blades over the threshold (C-1). These initial blades, however, were not functional due to the inadequate precision of the part files. Consequently, the final cost of the winglet and node blades doubled to total $22.80 and $29.73 respectively, accounting for the cost of printing a revised set of designs (C-1). Furthermore, the overall

expense attributed to each set of modified blades far surpassed the acceptable maximum cost outlined in the original specifications.

Experimental Set-Up:

To measure power output, the hub assembly was attached to a 12V DC gear motor utilized as a generator and mounted to a reinforced stand (Figure 6). This XD-3480 motor was specified according to the Chinese Compulsory Certification, defined by the GB Standards 12350 and 14711 specifically (Chinese Certification Corporation, 2017). The blades were subsequently secured to the hub with screws. Since the test section was not large enough to accommodate the blades, the apparatus was placed behind the wind tunnel to capitalize upon the airflow from the exhaust fan.

Figure 6: Testing stand with attached hub

The makeshift turbine was then subjected to increasing wind speeds, where five measurements for each blade were recorded as the wind tunnel speed varied from 45 mph to 65 mph. These wind speeds were measured for the area of the test section (11.5” x 12.5”), so the speed was adjusted to accurately represent the two-foot diameter of the exhaust airflow; the actual wind speeds ranged from 14 to 21 mph. A digital multimeter (DMM) was connected to the generator to record the voltage measurements in response to rotary motion. Since the input power was maintained through the constant wind speed across the trials, the variation in voltage was isolated to an increase in efficiency of the turbine.

According to the specifications, the ideal value for efficiency of the modified designs was zero reduction in efficiency, and the acceptable value was set at a 5% reduction (A-7). The test results indicated that the modified blades actually achieved a greater efficiency across most of the wind speeds compared to the base blade. More specifically, the serrations performed the best with an average 56.32% higher efficiency than the base blade (D-3). Although the jump in efficiency was theorized to be a result of an increase in surface area, a larger serration pattern was tested to verify that the measurements did not correlate with surface area. The smaller serrations actually performed better. Overall, the efficiency specification was achieved given that the other two modifications achieved an average 5.32% and 3.00% increase in efficiency that dropped off slightly at higher speeds (D-3).

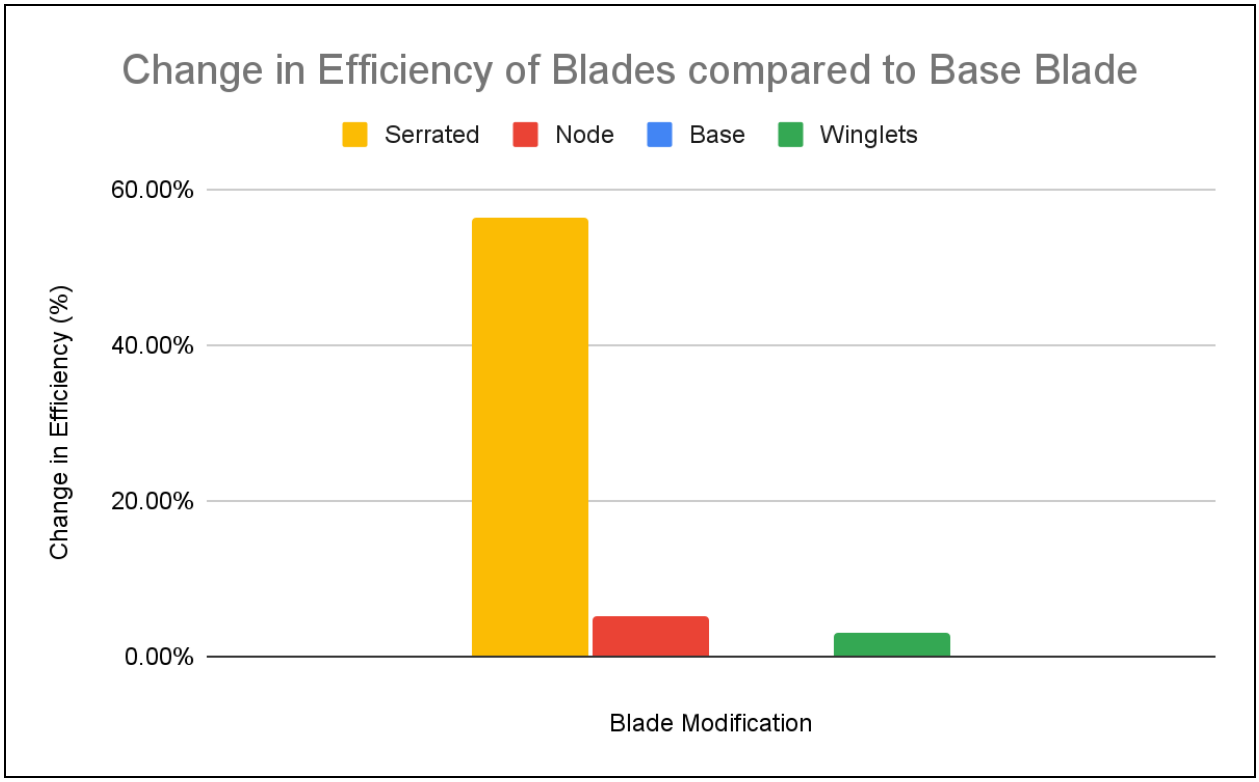

Figure 7. The percent difference in efficiency of the modified blades, where the base blade was used as a reference for comparison according to the specification metrics.

The sound mitigation modifications were verified through the measurement of noise loudness across the different blade designs. A power supply delivered a consistent 4.50 ± 0.05 V to the DC motor, simulating the operation of the wind turbine at a higher wind speed. The resultant low-frequency noise, a range from 20-200 Hz, was filtered through the Fast-Fourier-Transform (FFT) via the FFT Plot application in the App Store. To balance the tradeoff between the time and frequency resolution, the application was set to an FFT size of 4096 with fast averaging to capture the fluctuations of the rotary blades. An Apple EarPods microphone was positioned one inch above the blades along the vertical axis of the turbine to record the sound. The low sensitivity of the equipment combined with interference of the moving air-limited the measurements to this single location.

To meet the specification, the blades were projected to minimize the noise in comparison to the base blade by at least 2 dB with an ideal value of 8 dB (A-6). While a 3 dB decrease outside the laboratory is discernible, a 5 dB reduction typically results in a noticeable response from the general population (Hankard, 2019). Surprisingly, the winglet design was the only blade that failed to meet specifications, whereas the serrated trailing edge and noded blade both achieved acceptable noise reduction. The noded blade performed best with an average 5.69 dB reduction followed by the serrated blade with an average 3.31 dB reduction, whereas the winglet blade generated noise at approximately the same level as the base blade (D-7).

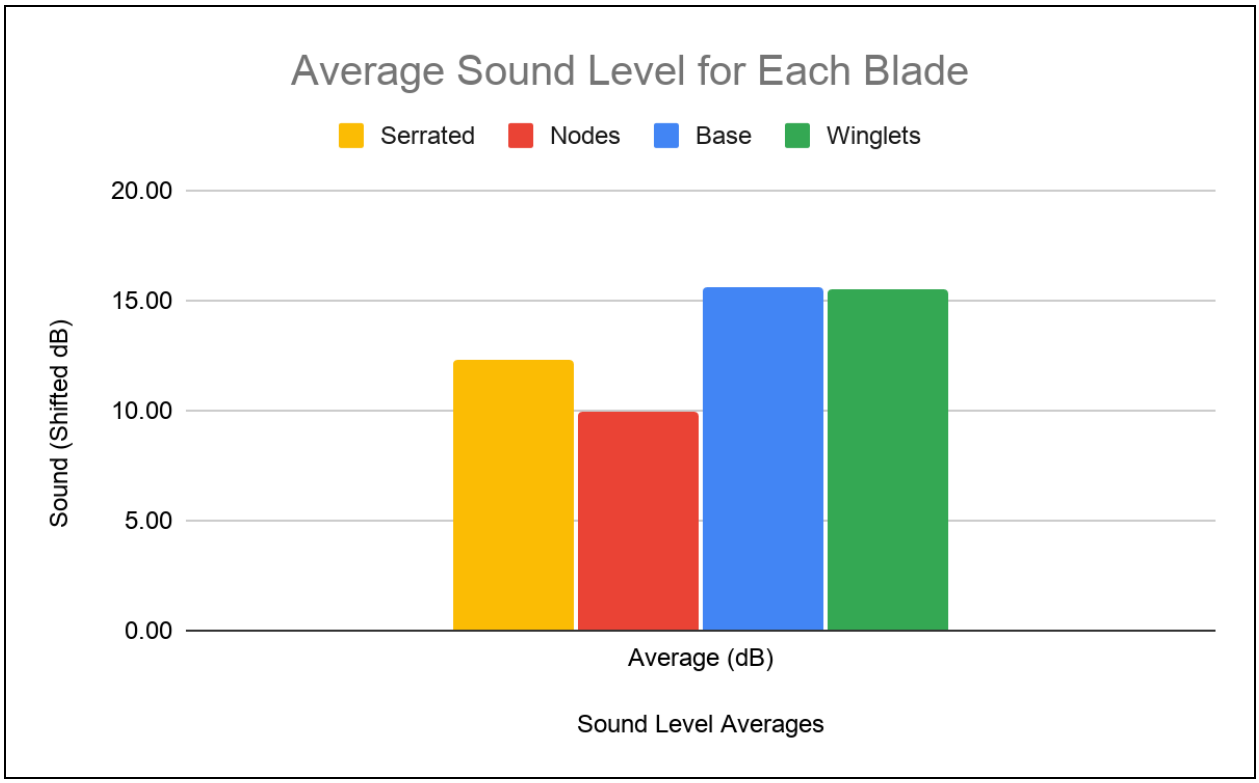

Figure 8. The average sound levels shifted to more clearly demonstrate the difference in noise production across the different blade modifications.

The sound measurements further revealed that the different blade modifications share approximately the same peak frequencies: 35, 76, 111, 146, 182, 223 Hz (D-4). Since the data predominantly falls within the low-frequency range, future design iterations should satisfy the

ANSI standard for noise assessment and long-term community predictions. More specifically, the standard specifies that the octave band sound pressure levels (dB SPL) should remain below 65 dB at the midband frequencies to maintain minimal community annoyance levels (Hankard, 2019). Moreover, the full-scale development of these rotor blades should be tested to ensure that they are in accordance with IEC 61400-11: Part 21 & 23 standards that concern acoustic measurement techniques and rotor structural testing (American National Standards Institute (ANSI), 2021).

COST ANALYSIS

Although turbine blade modifications show promise in noise mitigation, wide range acceptance and implementation depends on manufacturers, who must ultimately consider the cost of these alterations. When examining the serrated trailing edge and noded blade design, the modifications come with little added cost to the manufacturer. The serrations and nodes themselves require a small increase in raw material cost, however, fiberglass composite is relatively cheap. It costs approximately $2.00-$3.00 per pound (Cool Tech, 2020), and the modifications themselves are small in total volume. The machinability of the serrations does not come with many complications, as a waterjet, laser cutter, or hand tools could perform the simple 60-degree triangular cuts. Sculpting the nodes would require an additional mold, yet its design would be relatively straightforward. To attach the serrations and nodes to the base turbine blade, an adhesive would be applied at the interface, adding slightly more labor to the traditional process. Overall, the additional material and labor costs are relatively small, so it costs approximately an extra $500 maximum per blade after the initial investment of the node sculpting cast.

The winglet modification results in a higher manufacturing cost due to the complexity of the shape. Not only would the aforementioned material costs from an increased amount of fiberglass composite and adhesive apply, but the initial mold of the turbine blade would need to be reconstructed from scratch to incorporate the folded tip (Cool Tech, 2020). This redesign would require the skills of a design engineer and a precise laser measuring tool to ensure the correct curvature of the new cast. In comparison to the other designs, the winglet blade requires a much larger investment. The necessary cost of design engineer services and construction of a new cast costs roughly $100,000 to complete.

CONCLUSION

To optimize the rotor blades with the primary aim of sound mitigation, the team targeted the sources of aerodynamic noise with three separate blade designs. These modifications were tested experimentally using a small wind tunnel to determine the impact of the modifications on both noise production and power efficiency in comparison to a standard turbine airfoil. From these experimental results, the trailing and leading-edge modifications were proven to significantly reduce the overall noise in comparison to the control blade. Similarly, the blade with trailing edge serrations improved the turbine efficiency the most, whereas the other modifications increased efficiency only to a slight degree. Based on these results, the noded or serrated blade would be recommended for further development since they satisfied the two main specifications.

Although these results appear conclusive, the experimental design introduced multiple sources of error that may be improved in a number of ways. There were significant limitations to the scaled-down design that included the inability to test high wind speeds, the imprecision of the blade prints, and the use of a material with significantly different properties than fiberglass.

Additionally, the low sensitivity of the microphone combined with a small range of decibel levels somewhat undermines the conclusions drawn from the data. A full-scale model would produce a noise level that could be much more easily registered on measurement equipment, offering greater credibility to the data points since the values would be less likely to overlap within their uncertainty.

Moreover, there are numerous areas for future work with the development of sound-mitigating rotor blade designs. Given the significant increase in efficiency for the serrations, a deeper analysis of the surface area impact on the lift and drag force may provide further insight into the wind turbine aerodynamics. Additionally, the shared frequencies for each blade design could be further explored with the potential of developing modifications to target a specific frequency. The incorporation of all three modifications onto one blade has yet to be studied either. These studies are imperative given their insight into not only the technology itself but also its impact on public health. As the world grows to understand the negative implications of noise disturbance on local communities, it is the responsibility of design engineers to develop and implement quieter turbines to safeguard against potential harm.

References

Airfoil Tools. (2020). *NACA 2414 (n2414-il).* http://airfoiltools.com/airfoil/details?airfoil=n2414-il.

American National Standards Institute. (2021). *Wind Turbine Standards.* ANSI Webstore. https://webstore.ansi.org/industry/energy/wind-turbine.

Bai, C.J., Hsiao, F. B., Li, M. H., Huang, G.Y., Chen, Y. J. (2013). Design of 10 kW Horizontal-Axis Wind Turbine (HAWT) Blade and Aerodynamic Investigation Using Numerical Simulation. *Procedia Engineering, 67*, 279 – 287. https://doi.org/10.1016/j.proeng.2013.12.027.

BBC Earth. (2016, April 29). *Experiment! How Does an Owl Fly Silently* [Video]. Youtube. https://www.youtube.com/watch?v=d_FEaFgJyfA.

Buck, S., Oerlemans, S., & Palo, S. (2016, December 22). Experimental characterization of turbulent inflow noise on a full-scale wind turbine. *Journal of Sound and Vibration*, *385*, 219–238. https://doi.org/10.1016/j.jsv.2016.09.010.

Chinese Certification Corporation. (2017, June 6). *Chinese Compulsory Certification for Small Electric Motors.* https://www.china-certification.com/en/ccc-compulsory-certification-small-electric-motors/.

Cool Tech. (2020, June 25). *WIND BLADE TURBINE Manufacturing Process You Won't Believe How Are Made-Shocking Production Method* [Video]. YouTube. https://www.youtube.com/watch?v=hjv9g1tqGr8&t=186s

Council of Canadian Academies. (2015, April). *Understanding the Evidence: Wind Turbine Noise, The Expert Panel on Wind Turbine Noise and Human Health*. https://cca-reports.ca/reports/understanding-the-evidence-wind-turbine-noise/.

Deshmukh, S., Bhattacharya, S., Jain, A., & Paul, A. R. (2019, February). Wind turbine noise and its mitigation techniques: A review. *Energy Procedia*, *160*, 633–640. https://doi.org/10.1016/j.egypro.2019.02.215.

Hankard, M. (2019, November 21). Wind Turbine Noise Levels and Standards. *Western New York Wind and Health Forum.* https://static1.squarespace.com/static/5c34c6b685ede137995b2e5d/t/5de6c66083bec649d37bf425/1575405198113/Western+NY+Wind+Forum+Hankard+Noise+20191119.pdf.

Jianu, O., Rosen, M., Naterer, G. (2012, May 29). Noise Pollution Prevention in Wind Turbines: Status and Recent Advances. *Sustainability, 4,* 1104-1117. https://doi.org/10.3390/su4061104

Real Engineering. (2016, May 10). *Winglets - How Do They Work? (Feat. Wendover Productions)* [Video]. YouTube. https://www.youtube.com/watch?v=FNqXf6t7e-w

U.S. Energy Information Administration. (2020, October). *Short-Term Energy Outlook*. https://www.eia.gov/outlooks/steo/pdf/steo_full.pdf.

Williams, J. E. F., & Hall, L. H. (1970, March 9). Aerodynamic sound generation by turbulent flow in the vicinity of a scattering half plane. *Journal of Fluid Mechanics*, *40(04),* 657. https://doi.org/10.1017/s0022112070000368.

APPENDIX A
Project Ideation & Design

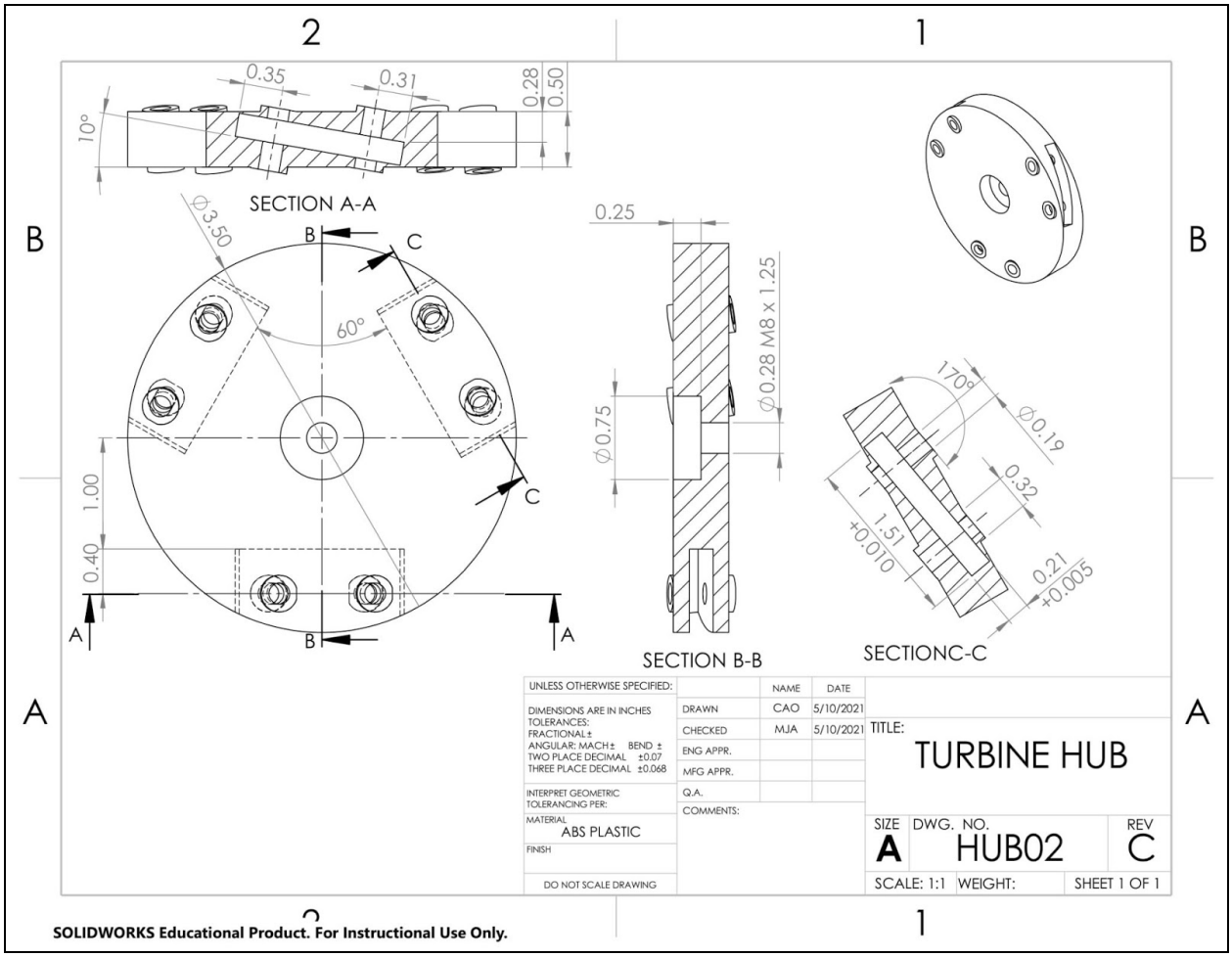

(A-1) Figure 9. Mechanical Drawing of the Turbine Hub (HUB02)

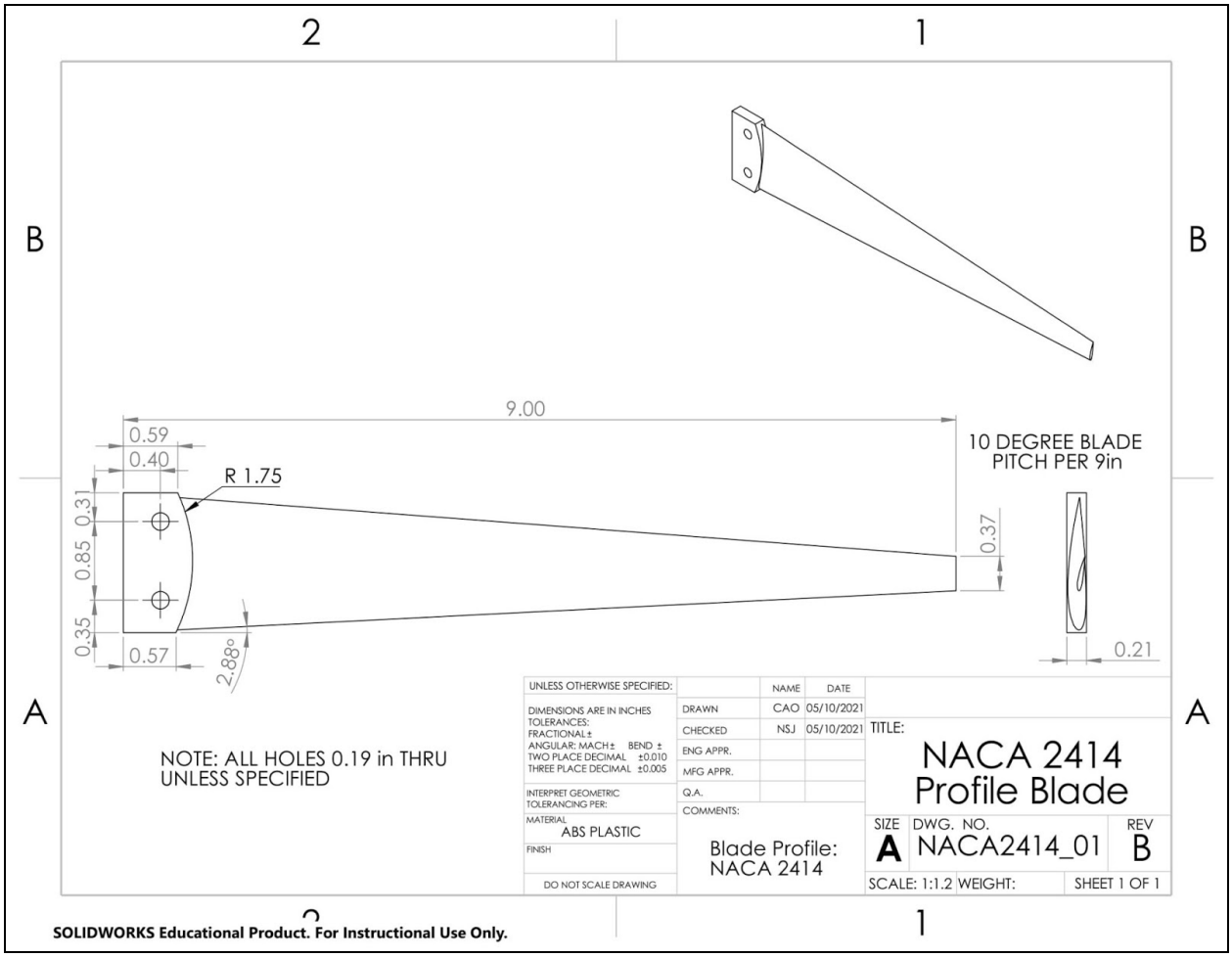

(A-2) Figure 10. Mechanical Drawing of the Base Blade (NACA2414_01)

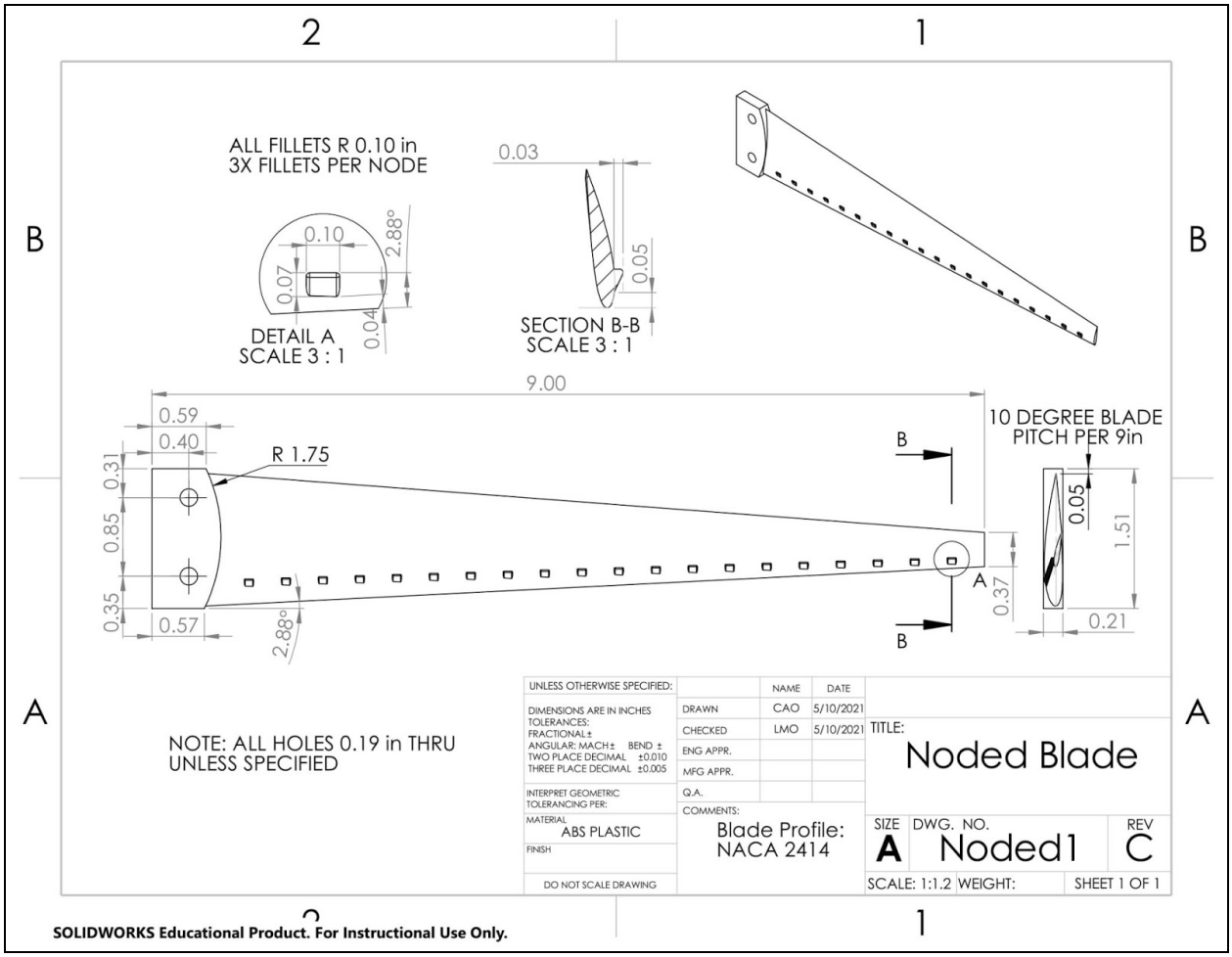

(A-3) Figure 11. Mechanical Drawing of the Noded Blade (Noded_01)

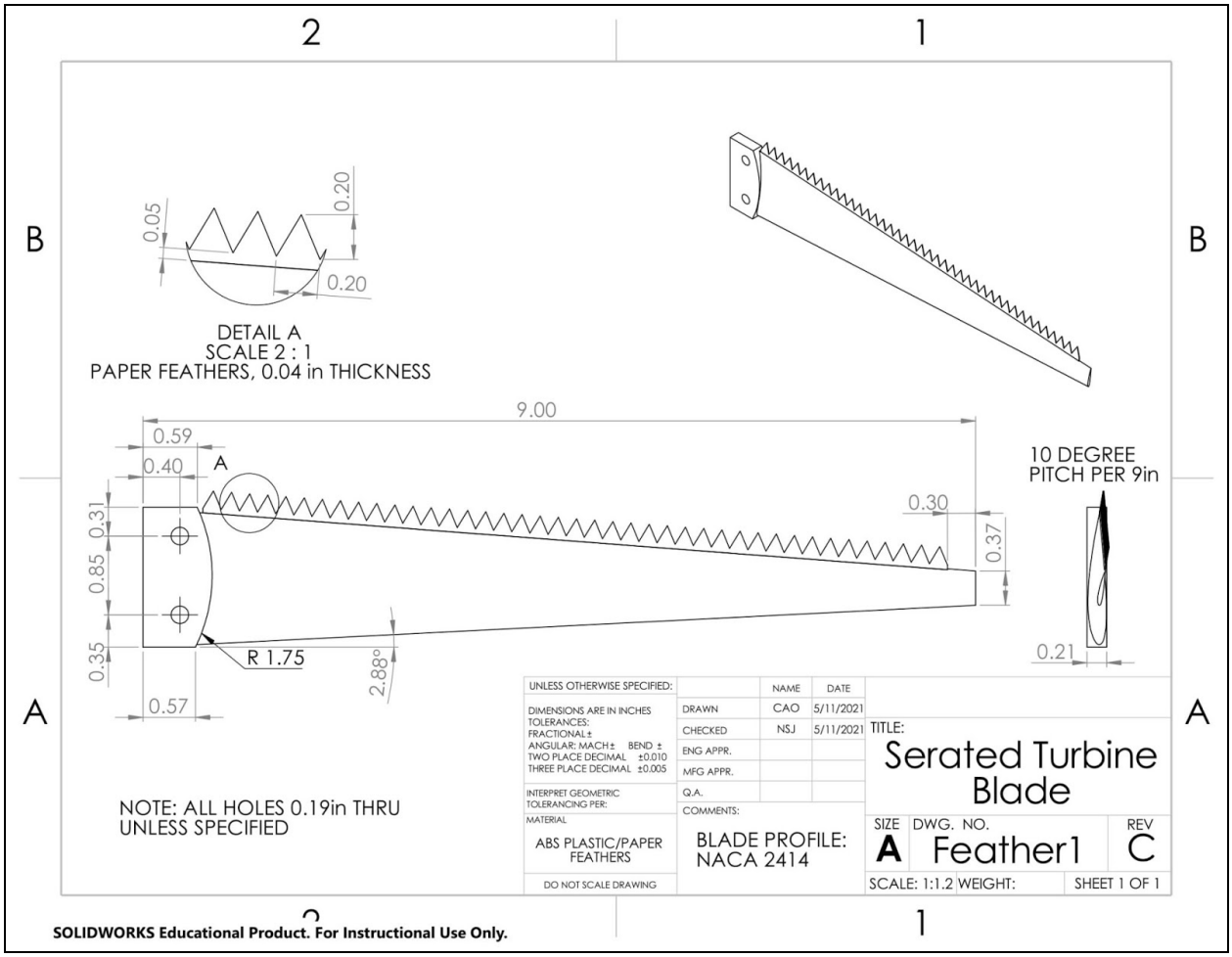

(A-4) Figure 12. Mechanical Drawing of the Serrated Blade (Feather1)

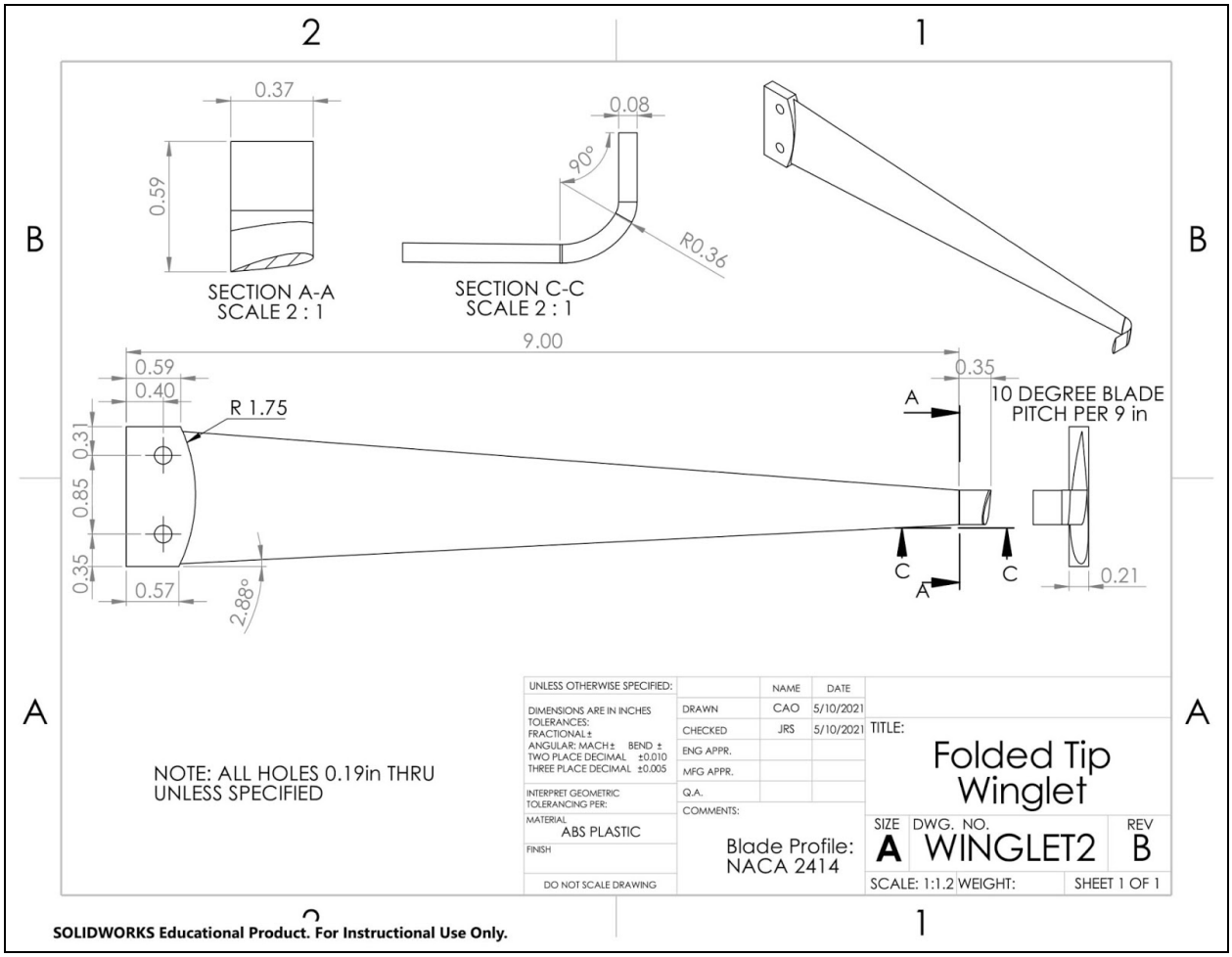

(A-5) Figure 13. Mechanical Drawing of the Folded Tip/Winglet Blade (WINGLET2)

(A-6)

Table 1. Sound Mitigating Blade Design Specifications

Modified Wind Turbine Blade Specifications				Reduction in Noise Production	Maintain Power Production and Efficiency	Low fixed cost addition to turbine	Durability/ can withstand high wind speeds	Easily manufactured
Metric	*Units*	*Acceptable*	*Ideal*	-	-	-	-	-
Modifying blade design (trailing edge, folded tip, noded surface)	dB	-2	-8	**X**				
Modifications to design largely to not affect efficiency	%	-5	0		**X**			
Blade able to sustain large wind speeds	mph	35	40				**X**	
Blade able to sustain large rotational speeds	rpm	12	20				**X**	
Modifications do not increase cost of blade manufacturing	%	5	0			**X**		X
Modifications do not inhibit time to manufacture	days	2.25	2			**X**		**X**

APPENDIX B
Calculations

(B-1)

Table 2: Input Values for Solidworks Simulations

Variables	Values
Air Density (at 20 C, 1 atm) kg/m^3	1.204
Wing surface area (m^2)	0.304
Wind Velocity 1 (m/s)	17.88
Drag Force 1 (N)	2.34
Wind Velocity 2 (m/s)	53.65
Drag Force 2 (N)	21.05

(B-2)

Table 3: Maximum Stress and Deflection Simulation Results

	Maximum Deflection 1 (mm)	**Maximum Stress 1 (MPa)**	**Maximum Deflection 2 (mm)**	**Maximum Stress 2 (MPa)**
Base Blade	2.44	0.492	11.20	0.464
Noded Blade	1.66	0.057	14.91	0.516
Serrated Blade	1.66	0.068	35.06	14.750
Folded Tip Blade	0.13	0.355	125.80	3.158

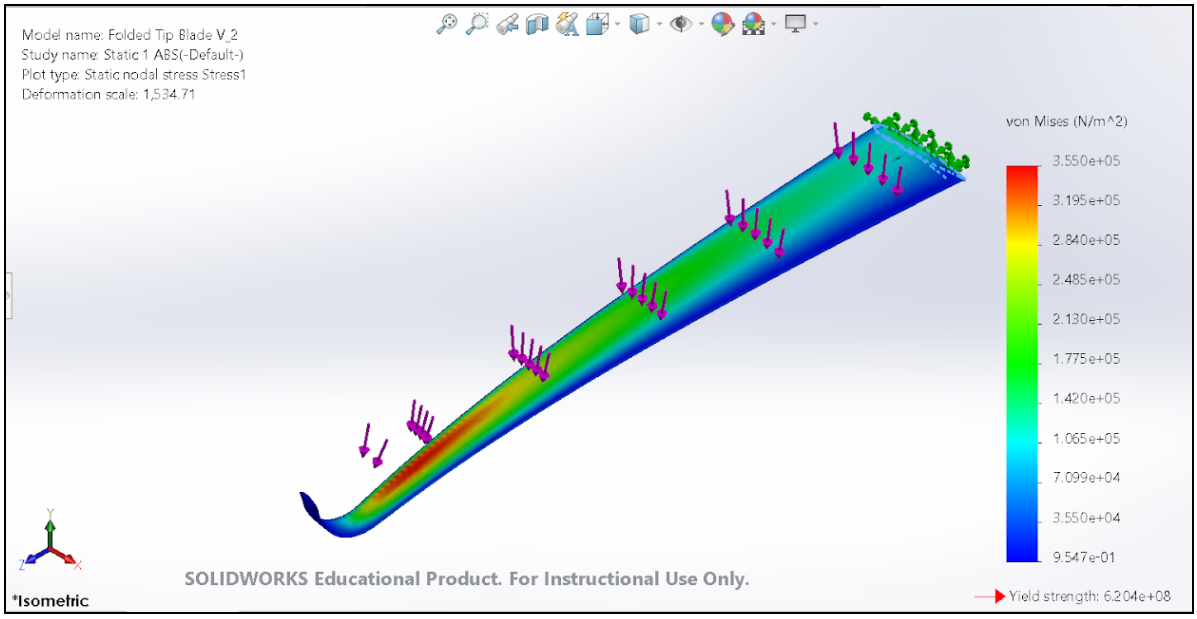

(B-3) Figure 14. Stress Simulation of Winglet Blade subject to 40 mph wind with a 0.134 mm maximum deflection.

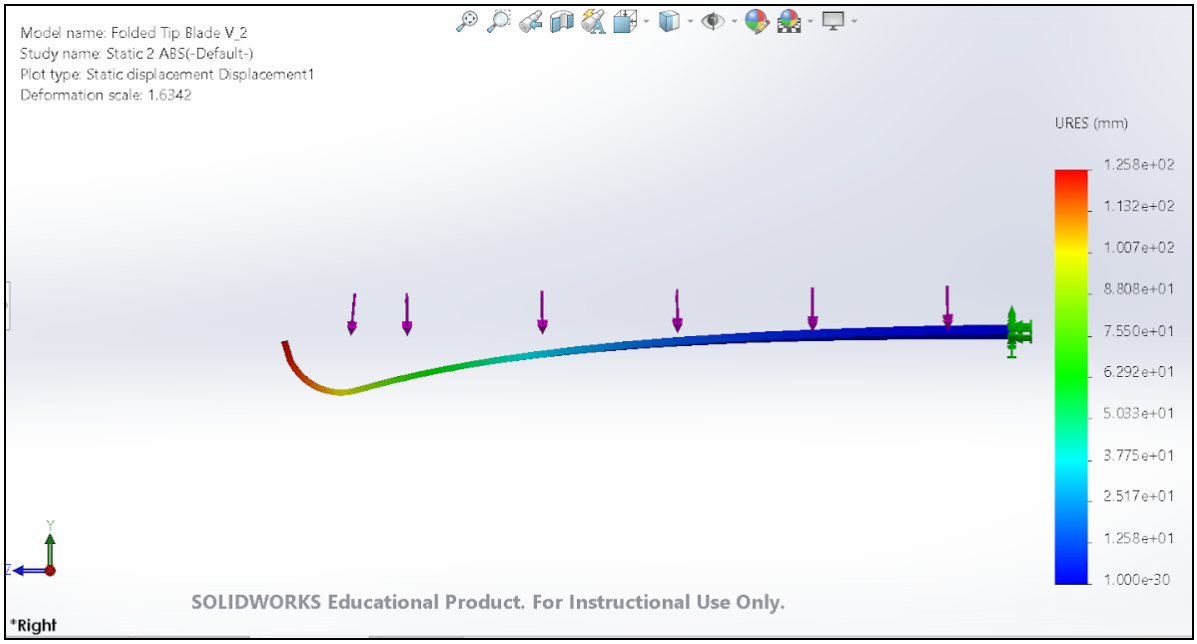

(B-4) Figure 15. Deflection Simulation of Winglet Blade subject to 120 mph wind with a 0.3158 MPa maximum stress.

(B-5)

Table 4. Input and Output Values for Maximum Angular Speed Calculations

Area (m^2)	0.01626
Mass (kg)	7.60
Stress, Sy (MPa)	30
Radius	1.83
Critical Force (kN)	487.74
Acceleration (m/s^2)	64176.70
Tip Velocity (m/s)	484.49
Max Wind Speed (m/s)	80.75
Max Wind Speed (mph)	180.63
Max Angular Speed (rpm)	2529.84

APPENDIX C
Project Cost Analysis

(C-1)

Table 5. Overall Cost of Blade Fabrication in Comparison to Specification

	Base Blade	**Serrated Blade**	**Noded Blade**	**Winglet Blade**
Initial Set (3)	$14.31	$18.90	$17.16	$14.04
Additional Prints	N/A	N/A	$12.57	$8.76
Total Cost	14.31	$18.90	$29.73	$22.80
Percent Difference	N/A	32.08%	108.8%	59.33%

APPENDIX D
Experimental Data & Results

(D-1)

Table 6. Raw Efficiency Data

Output Speed (mph)	45	50	55	60	65
Actual Speed (mph)	14.3	15.9	17.5	19.1	20.7
Serrated (Volts)	2.06	2.37	2.62	2.81	3.02
Node (Volts)	0.91	1.38	1.71	2.03	2.34
Base (Volts)	0.27	1.24	1.63	2.01	2.26
Winglets (Volts)	1.04	1.41	1.67	1.98	2.2

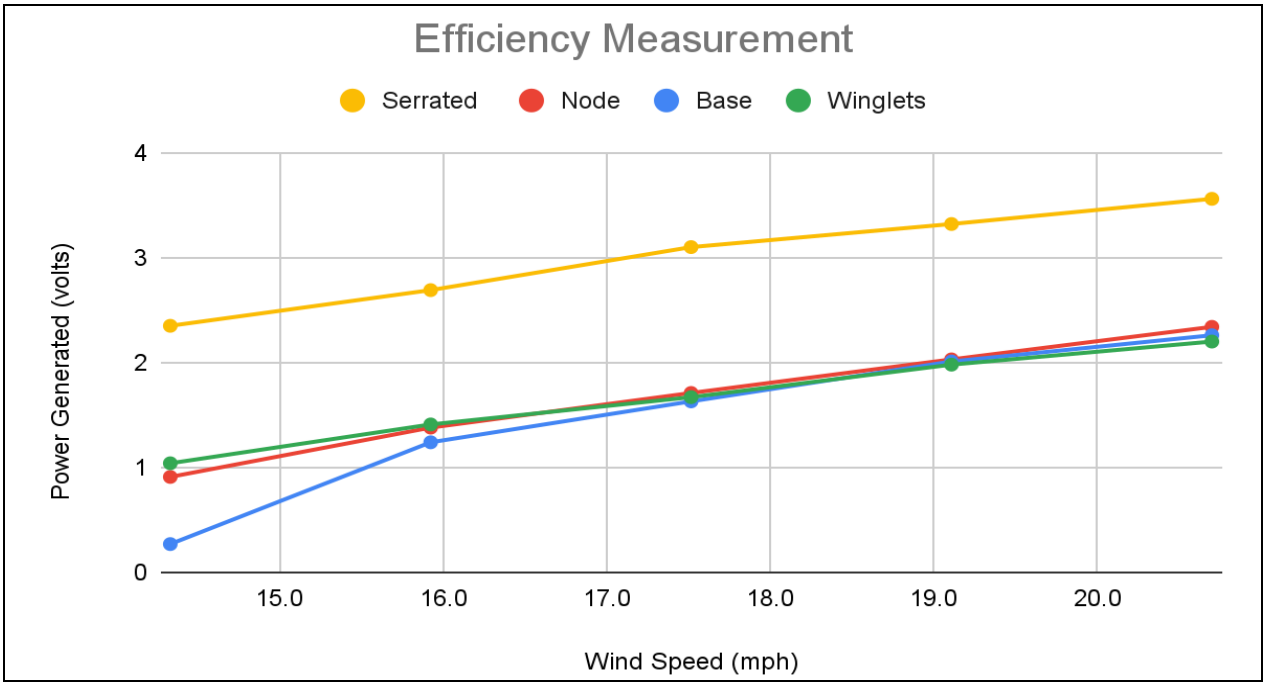

(D-2) Figure 16. The efficiency of each set of blade designs represented by the output voltage generated from the rotor rotation at varying wind speeds.

(D-3)

Table 7. Average Change in Efficiency of Sound-Mitigating Blade Design

Test Speed (mph)	50	55	60	65	Average Efficiency Difference
Actual Speed (mph)	15.9	17.5	19.1	20.7	
Serrated	91.13%	60.74%	39.80%	33.63%	56.32%
Node	11.29%	4.91%	1.00%	3.54%	5.18%
Base	0.00%	0.00%	0.00%	0.00%	0.00%
Winglets	13.71%	2.45%	-1.49%	-2.65%	3.00%

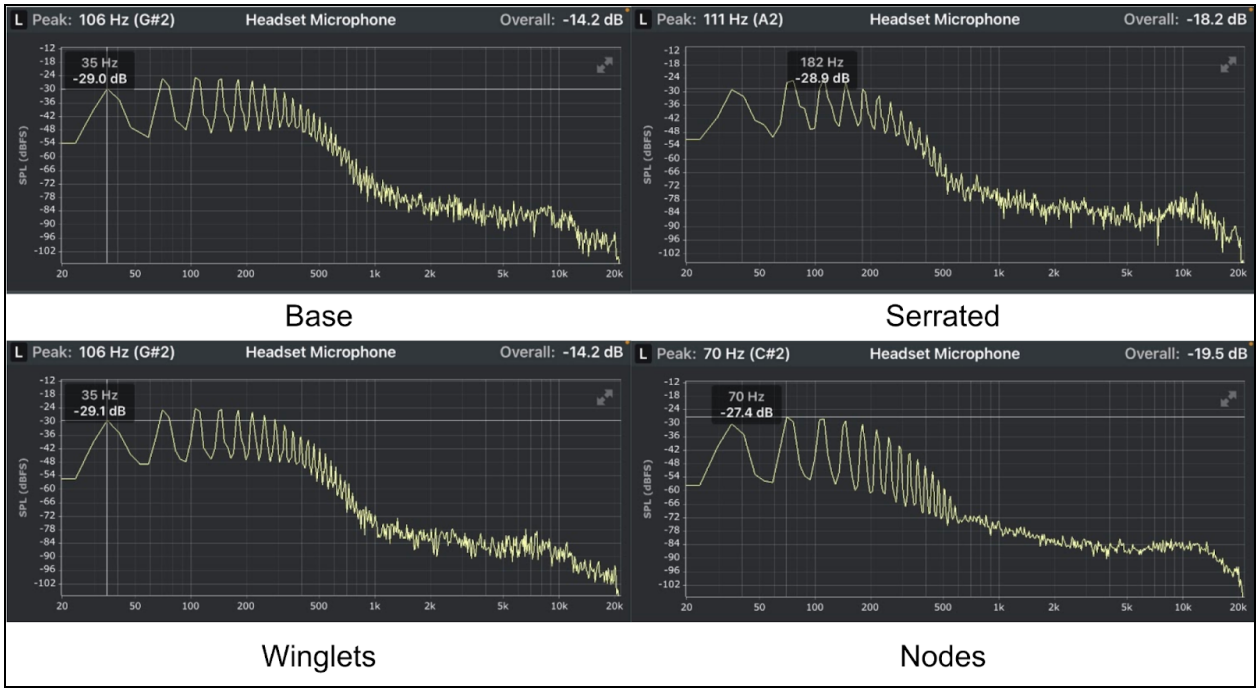

(D-4) Figure 17. Snapshots of FFT plot data collection timeframe for each blade.

(D-5)

Table 8. Raw Sound Level Data

Sound Levels (dB SPL)														
Serrated	-21.4	-20.5	-18.2	-16.9	-17.4	-17.3	-18.2	-18.1	-17.3	-16.8	-16.5	-16.7	-16.5	-16
Nodes	-19.6	-20.3	-20.2	-20.3	-20.2	-19.9	-19.2	-19.8	-20.1	-19.9	-20.5	-20.7	-20.4	-20
Base	-15.5	-14.2	-13.3	-13.1	-12.8	-13.1	-13.5	-14.5	-15.3	-15.1	-15.3	-15.2	-15.4	-15.1
Winglets	-16.5	-15.9	-14.5	-14.2	-14.3	-14	-13.9	-13.4	-13.5	-13.8	-14.4	-14.5	-14.9	-14.7

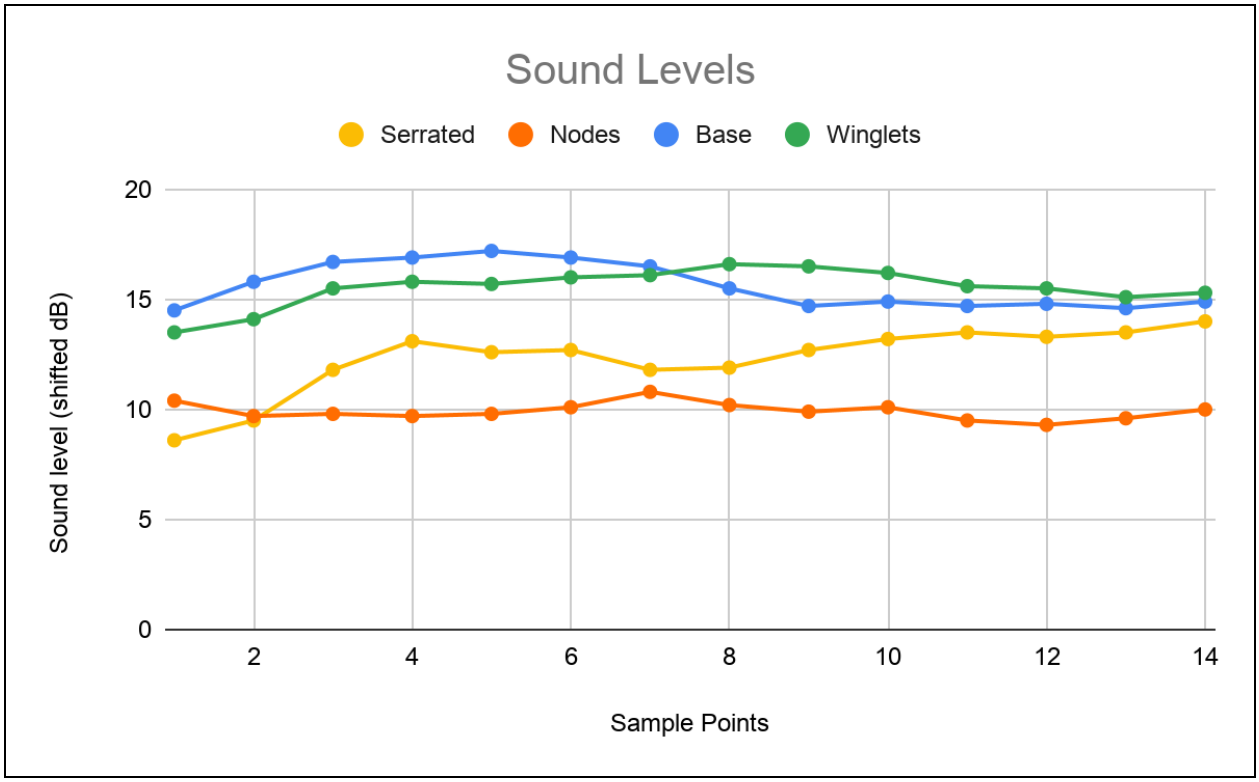

(D-6) Figure 18. The shifted sound levels for fourteen discrete data samples over the trial run period. Since the sound levels were less than the reference level, the raw data was shifted upwards to more clearly demonstrate the difference in volume across the designs.

(D-7)

Table 9. Average Sound Level Results for each Blade Modification

Blade	Serrated	Nodes	Base	Winglets
Average (dB)	12.30	9.92	15.61	15.54
Difference (dB)	-3.31	-5.69	0.00	-0.08
Difference (%)	-21.23%	-36.46%	0.00%	-0.50%

APPENDIX E
Miscellaneous

(E-1)

Group Members and Roles

Megan Anderson: Introduction/Report Editor
Levi Otis: Data Analysis/Appendices
Caleb Owen: Drawings/Background
Nathan Jacobson: Cost Analysis/Conclusion
Justin Smith: Specifications